ON STREAM INHOMOGENEITIES IN A PULSED ELECTROMAGNETIC ACCELERATOR

A. M. Rushailo

In a number of papers [1-7] carried out on various pulsed electromagnetic accelerators the appearance of a lamellar structure in the stream of accelerated ionized gas occurs having an oscillation frequency of several megahertz. The majority of authors relate the development of irregularities in the stream with local peculiarities in the flow of electric currents (secondary breakdowns [6], the formation of micropinches [3-5], the motion of a current spiral [2], etc.). Notwithstanding the generality of many properties of the irregularities recorded under various conditions, no unified point of view exists as yet concerning the nature of their development.

The present paper reports on methods of split photoscanning for carrying out an experimental investigation of certain peculiarities of the development of stream irregularities in a coaxial erosion accelerator. Based on the experimental data, the assumption is stated that the electromagnetic end effect influences the appearance of the irregularities. It is shown that planar irregularities having an axisymmetric shape appear in the zones of stream retardation behind the end shock wave and near the surface of the electrodes at the end of the accelerator channel.

The influence of deadsorption and evaporation from the surface of the electrodes on the development of the irregularities is noted. Experiments were carried out on the artificial excitation of deep and stable irregularities by retarding the stream in the zones of intense evaporation of the insulator.

1. The experiments were carried out on an apparatus partially described in [8, 9]. The basic parameters of the apparatus were: capacitance of the capacitor bank 1480 μF; initial inductance 50 nH; pressure in the working chamber (2 to 5) $\cdot 10^{-5}$ mm Hg. The energy reserve in the capacitors varied in the range from 6.6 to 18.5 kJ at a voltage of from 3 to 5 kV. The characteristic accelerator operating time (a half-period of the discharge) was 35 to 40 μsec, while the maximum values of the total current ranged up to 450 kA. The form of discharge was close to aperiodic.

The working substance consisted of the material produced by the erosion of a teflon insulator and partially the material produced by erosion of the copper accelerating electrodes. The teflon insulators

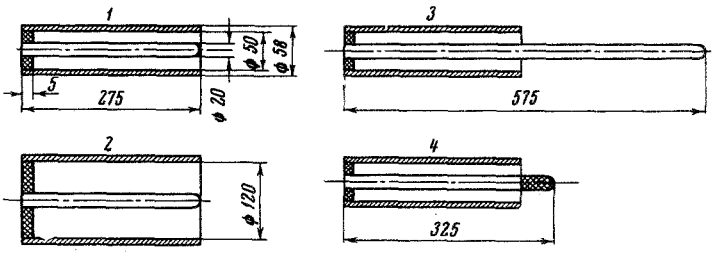

Fig. 1

Moscow. Translated from Zhurnal Prikladnoi Mekhaniki i Tekhnicheskoi Fiziki, No. 4, pp. 143-149, July-August, 1970. Original article submitted February 4, 1970.

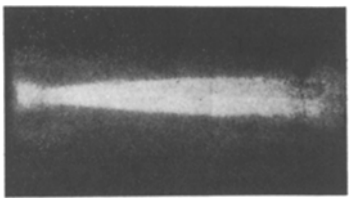

Fig. 2

simultaneously serve as a discharge stabilizer in the initial sector of the cylindrical channel.

From integral-measurement data (a combined pendulum-calorimeter, spectroscopy, weighing, streak photography, etc.) during one discharge a mass of working substance ranging from 1 to 6 mg was accelerated to velocities of 60-80 km/sec. The characteristic density of the particles in the stream was in the 10^{15}-10^{17} cm^{-3} range, while the electron temperature was of the order of $3 \cdot 10^4$°K [10].

The apparatus operated in a "gated"-voltage mode. The discharge was initiated by a high-voltage pulse from an SFR streak camera which had been power-amplified by the discharge of a 1 μF capacitor at a voltage of 2 to 5 kV.

The diagram and dimensions of the accelerating electrodes used in the experiments are shown in Fig. 1. In a number of cases four apertures 1 cm in diameter were made in the outer electrode, which were uniformly spaced along the electrode length. The extreme apertures were situated at a distance of 1 cm from the insulator and from the muzzle of the electrodes.

Slit scanning was accomplished by the SFR streak camera. For a slit width of 0.05-0.1 mm and a mirror rotation speed of from 45,000 to 90,000 rpm (the velocity of the light beam on the photographic film ranged from $2.25 \cdot 10^5$ to $4.5 \cdot 10^5$ cm/sec) the time resolution of the system amounted to 10-50 nsec. The investigations were carried out for a horizontal (along the stream) and vertical (across the stream) orientation of the slit. The linear image-reduction coefficient was equal to 3.

The magnetic field in the accelerator was measured by coil magnetic probes placed in a quartz tube [11]. Magnetic probes having an ellipsoidal shape with dimensions $6 \times 3 \times 2.5$ mm were used. The probes consisted of 80 turns of copper wire 0.08 mm in diameter and had an inductance of 1.5 μH. For a sensitivity of $5 \cdot 10^{-5}$ V/G the magnetic probes allowed field oscillations having a frequency of up to 30 MHz to be recorded without noticeable distortion. The signal from the magnetic probe was integrated by a RC circuit and recorded by an OK-17M oscilloscope.

2. In the accelerator the considered time for which an accelerated particle remained inside the channel was one order shorter than the discharge time; therefore, in a well-known sense the flow could be assumed quasistationary. The accelerated ionized gas undergoes the application of an electromagnetic and gasdynamic applied force at the accelerator muzzle, which leads to a rotation of the stream toward the axis and the formation of an oblique compression shock. The end effects were considered theoretically in [12].

Ahead of the shock wave the main stream produces a weak luminescence. An increase in the temperature behind the compression shock leads to an abrupt increase in radiation and allows the stream to be recorded by means of streak photography. Figure 2 shows a photograph obtained behind the accelerator muzzle using an SFR streak camera with an exposure time of 0.6 μsec. On the photograph the cone-shaped shock wave which develops in the stream as a result of the flow past the inner electrodes is well visible. The shock wave caused by the end effect was observed for all of the accelerator models considered here and in all of its operating modes.

Slit scanning increased the time resolution and allowed it to be revealed that the flow in the zone behind the shock wave is inhomogeneous. Figure 3 shows vertical slit sweeps 1, 2 taken for accelerator model 1 at distances of 1 and 10 cm from the accelerator muzzle. The direction of the sweep and the flow velocity is from left to right here. Sweep 1 in Fig. 3 was obtained for a mirror speed of rotation equal to 90,000 rpm, while the remaining sweeps shown in the paper were obtained at a speed of 45,000 rpm. From sweep 2 (Fig. 3) it is evident that the flow behind the shock wave has a lamellar structure with waves having a shape close to planar. The processing of numerous experiments showed that the frequency of the light irregularities in the zone behind the shock wave is in the range from 5 to 20 MHz. For a stream velocity of $6.5 \cdot 10^6$ cm/sec the wavelength of the irregularities (the distance between two planar formations having an elevated luminosity which follow one another) is from 3 to 13 mm.

The lamellar structure of the flow behind the end shock wave was recorded at various distances from the ends of the electrodes and in all operating modes of the accelerator.

The vertical sweep of the stream 1 in the immediate vicinity of the muzzle (1 cm) shows (Fig. 3) that in a stream flowing out into the shock-wave zone there are layers having an inhomogeneous structure. These

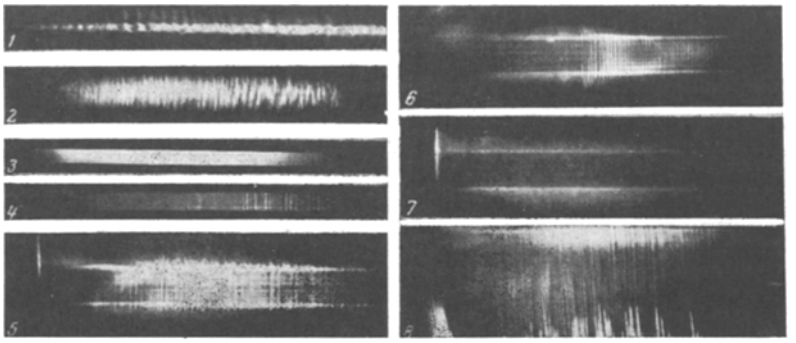

Fig. 3

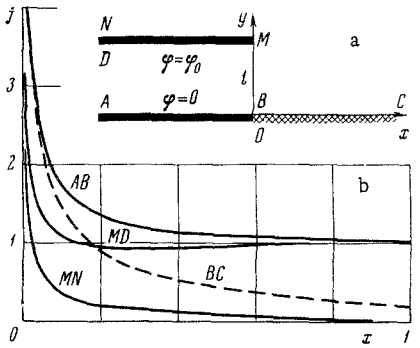

Fig. 4

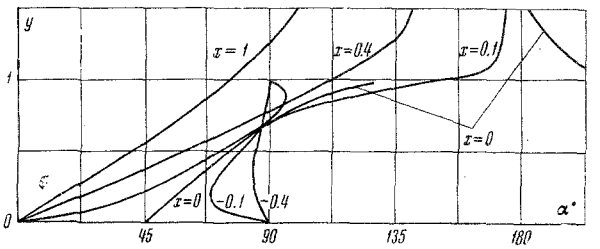

Fig. 5

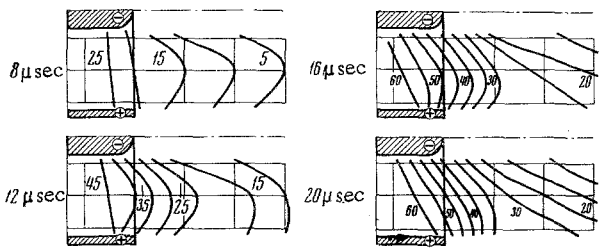

Fig. 6

layers, which have a thickness of several millimeters, appear inside the accelerator channel and run off from the surface of the inner electrodes.

Figure 3 shows the vertical stream sweep 5 obtained directly at the accelerator muzzle 1 by photographing at a small angle between the optic axis of the SFR and the muzzle plane. The surface of the inner electrode and a portion of the inside surface of the outer electrode were within the field of view of the SFR slit. From the sweep 5 (Fig. 3) it is evident that in a narrow zone next to the inner electrode plane waves having a frequency of the order of 5 MHz develop a short time after the beginning of the discharge.

Sweeps taken through apertures in the outer electrode showed that there are no irregularities inside the channel. In order to illustrate this Fig. 3 shows a vertical sweep 3 taken from the first aperture (1 cm from the insulator) of model 1 having a resolution up to 50 MHz.

The fourth aperture (1 cm from the muzzle) is an exception. The sweep 4 taken through this aperture showed that the stream becomes inhomogeneous at the end of the accelerator channel (Fig. 3).

The three vertical sweeps 5, 6, 7 taken under identical conditions in three successive experiments at a small angle on the accelerator muzzle 1 (Fig. 3) show that the time delay of the appearance of irregularities near the inner electrode at the end of the channel varies from experiment to experiment. This effect is considered at the end of the present paper.

A characteristic horizontal slit sweep 8 of the stream at the exit from the accelerator is likewise shown in Fig. 3. The slit of the SFR was situated at a distance of 1.2 cm from the accelerator axis at the level of the luminescent near-electrode layer. The direction of the sweep was from left to right, and the direction of the stream velocity was from the top down.

From the SFR photogram it is evident that the irregularities move together with the stream at a velocity of 60 to 80 km/sec while retaining their stability over the entire visible displacement path. In the zone of the end shock wave the brightness of the irregularities increases abruptly.

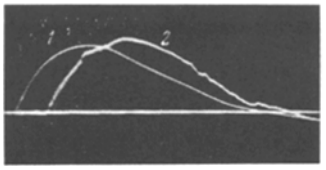

Fig. 7

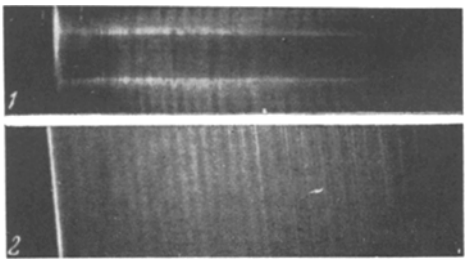

Fig. 8

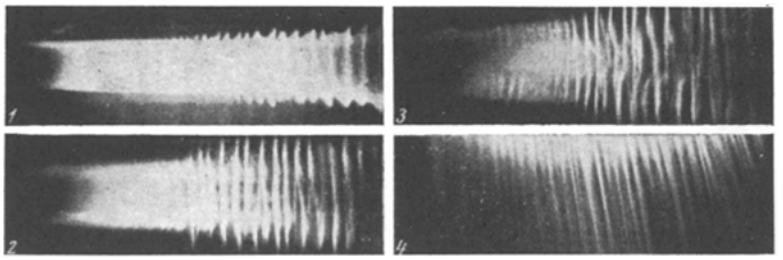

Fig. 9

Existing theories of the lamellar structure of the flow in pulsed accelerators cannot explain the experimental results given here to a sufficient degree. The theory of repeated breakdowns on the insulator behind a moving current front [6] is inapplicable, since no irregularities were observed in the initial sector of the channel. The theory of spiral flow of electric current [2] likewise cannot explain the flow pattern, since the irregularities usually have a proper planar form which is well preserved in the flow for a prolonged period. For the same reasons the explanation that the irregularities considered here are generated by cutoffs of the current micropinches [3-5] likewise seems improbable.

The end effect, which is expressed in a departure of a portion of the electric current beyond the limits of the accelerator, leads to the formation of a shock wave. However, the electromagnetic end effect extends over a certain distance into the interior of the channel also. The possible deviation of the current lines from the radial direction inside the channels must lead to the appearance of a radial component of the electromagnetic force which compresses the plasma against the electrodes. Similarly to oscillations of the luminosity behind the end shock wave, the nonuniformity of the stream at the end of a coaxial channel may be related to the gasdynamic condensation of the stream at the surface of the electrodes due to the end effect. This assumption allows the appearance of irregularities solely at the end of the channel in a narrow zone near the electrode to be explained.

In order to substantiate the assumptions stated, certain estimates and special experiments were performed.

3. In order to estimate the penetration depth of the end effect into the interior of the coaxial channel, the degree of slope of the lines of electric current toward the axis, and the various distribution patterns of the current lines at the inner and outer electrodes, the model electrostatic problem of the distribution of electric current between two planar semi-infinite ideally conducting electrodes (a continuation of one of these electrodes is the insulator; Fig. 4a) was solved. The conductivity of the medium in the half-space $y > 0$ is assumed constant.*

The problem was solved by the method of conformal mappings [14]. The absence of a tangential current component on the electrodes and the absence of a normal current component on the insulator were adopted as boundary conditions.

Certain results of solving the model problem are displayed in Figs. 4b and 5.

*The problem stated is a combination of two classical problems involving a capacitor and the current distribution in a channel with planar electrodes and insulating barriers [13].

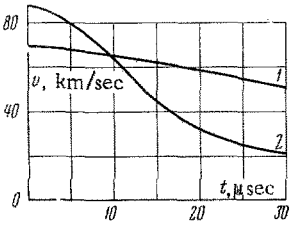

Fig. 10

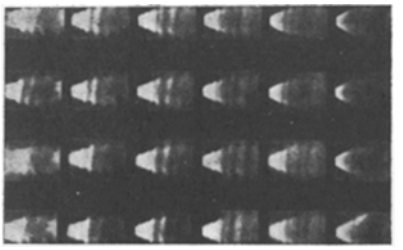
Fig. 11

Figure 4b is the diffusion of the absolute magnitude of the current on the surface of the electrodes and of the insulator. The dimensionless magnitude of the current $j = j_* \cdot l/\varphi_0$ is plotted along the axis of ordinates, while the modulus of the dimensionless coordinate $x = |x_*|/l$ is plotted along the axis of abscissas; here l is the distance between electrodes, while φ_0 is the potential difference. The asterisk denotes dimensioned quantities.

It is evident that the end effect on the surface of the electrodes penetrates into the interior of the channel to an amount which is of the order of one gauge.

Figure 5 shows the dependences of the slope angle of the electric current lines ($\operatorname{tg} \alpha = j_x/j_y$) on the dimensionless coordinates $y = y_*/l$ with the x-coordinate as the parameter. From the graph it follows that the pattern of the current lines is nonsymmetrical. The slope of the current near the lower electrode is several times more pronounced than it is near the upper electrode. The minimum slope angle of the current lines inside the channel is 45°.

The model problem shows that the end effect extends into the interior of the channel to a depth of several channel widths and is manifested near the surface of the lower electrode (near the inner electrode in the case of a coax) several times more intensively than at the surface of the upper (outer) electrode. Consideration of the flow of the conducting medium, the magnetic field, and the counter-emf, just as consideration of the two-dimensional nature of the flow in a coaxial channel, must merely intensify the dependences noted.

The estimate which is carried out and the assumptions which are made allow us to explain why the irregularities appear only at the end of the channel and are manifested considerably more strongly near the inner electrodes and weakly at the surface of the outer electrode.

4. The measurements performed on model 2 by means of magnetic probes showed that the discharge and the magnetic field in an accelerator have good azimuthal symmetry, while the magnetic probe does not introduce substantial distortion into the current and magnetic field distributions. Under these conditions the longitudinal and radial distributions of the magnetic field in the region of the accelerator muzzle were used to construct an approximate picture of the current loss. The pictures of the current lines for several characteristic lines are displayed in Fig. 6. The lower region of the accelerator muzzle relative to the axis is shown. The numbers indicate the magnitude of the current flowing to the right of the current line. The current lines were found on the assumption of a linear variation of the field between two neighboring measurement points. The distances between measurement points were 3 cm along the axis and 2 cm along the radius.

From Fig. 6 it is evident that as a whole the experimenters found patterns of the current lines to be in good agreement with the estimates performed above. Actually, the steep slope of the current lines is observed not only behind the accelerator muzzle but also at a certain distance into the interior of the channel.

Figure 7 shows a characteristic oscillogram for the total current 1 and a magnetic field 2 at a point situated on the accelerator muzzle 1.6 cm from the axis. The initial voltage is 3 kV; the maximum values of the current and magnetic field on the oscillogram are 170 kA and $5 \cdot 10^3$ G, respectively. A half-cycle of the current on the oscillogram amounts to 37 μsec. Notwithstanding the high-quality frequency characteristics of the magnetic probe and the placement of the probe directly in the zone of appearance of the irregularities, the oscillogram of the magnetic field does not have high-frequency oscillations with a noticeable modulation depth. The absence of substantial oscillations of the magnetic field may serve as an indirect substantiation of the fact that the irregularities in the experiments concerned are not associated with strong current fluctuations.

5. The assumption of the influence of the end effects on the development of irregularities inside the channel was checked in the following experiment. Using a model having an outer electrode 27 cm long and an inner electrode 57 cm long (model 3), the slope of the current lines at the surface of the inner electrode in the region of the muzzle must be practically nonexistent. The end effect must be manifested near the surface of the outer electrode more abruptly in this model. In fact, the vertical slit sweep 1, as obtained for a small angle on the muzzle of the outer electrodes, and the horizontal sweep 2 taken at the output above the surface of the inner electrode (Fig. 8) show that irregularities which develop at the outer electrode were noticeably intensified, while they were reduced at the inner electrode. The frequency of the oscillations in the outer and inner zones amounted to 1.1 and 4.5 MHz, respectively, for an average rate of displacement $7 \cdot 10^6$ cm/sec. Consequently, the distance between irregularities in the outer and inner zones of the stream is different and amounts to 6 and 1.5 cm, respectively.

Superimposed oscillations at two different frequencies are visible on the horizontal slit sweep, since both near-electrode regions fall in the field of the slit simultaneously.

The gasdynamic and electromagnetic rotation of the stream at the exit from the channel at the inner electrode is absent by virtue of the specific features of the model; therefore, outflow, as is also evident from the SFR photogram, takes place without the formation of an end shock wave.

6. As was shown above, the laminarity of the stream in the near-electrode zone changes from discharge to discharge. With an increasing number of starts of the apparatus the intensity of the irregularities decreased, the time delay in their appearance increased, and in a number of cases the irregularities vanished entirely (Fig. 3).

The result noted may be explained by deadsorption of residual gases and vapors of vacuum oil from the surface of the electrodes during the process of electrode heating [8]. An indirect substantiation of deadsorption lies in the fact that in the initial experiments after a prolonged break the pressure in the working chamber exceeds the pressure which develops in the chamber in subsequent experiments by one order. The deadsorption has a noticeable effect on the integral characteristics also, reducing the energy efficiency by 20 to 30% and increasing the accelerator pulse in the first experiment by 40 to 50%.

The assumption that deadsorption and vaporization affect the development of irregularities was made the basis of the experiment on artificial intensification of the irregularities.

The inner accelerator electrode was extended by means of an insulating adapter (Fig. 1, model 4). The adapter material was Plexiglas, Teflon, or aluminum oxide.

High densities of the electric current on the electrode-adapter interface led to a considerable erosion of the insulator. According to weighing data the mass of insulator evaporating in one discharge amounted to a magnitude comparable to the mass of the working substance accelerated under ordinary conditions.

The experiment with an insulating adapter was the continuation of an experiment with an elongated inner electrode. Besides increasing the erosion, the purpose of separating the electromagnetic and gasdynamic rotations of the stream at the exit from the accelerator was pursued. It is clear that basically electromagnetic forces act on the stream in the region of the electrode-adapter interface; these forces must press the stream against the surfaces of the electrode and the adapter due to the end effect and thus cause the appearance of a shock wave. The gasdynamic rotation of the stream must occur independently of the electromagnetic rotation at the end of the insulator.

The results of the experiment with a Plexiglas adapter are presented in Fig. 9. The numbers 1, 2, and 3 show the vertical slit sweeps taken at distances of 2.5, 4.5, and 6.5 cm from the end of the inner electrode, while the number 4 indicates the horizontal slit sweep taken at a distance of 0.3 cm from the insulator surface. The initial voltage was 5 kV.

From the SFR photograms it is evident that in a narrow cylindrical zone at the insulator surface a bright flow region develops behind the end of the shock wave. For the first 10 to 15 μsec the flow remains uniform. Then plane waves having a frequency of 0.5 to 1.5 MHz develop in the near-wall stream, which move in a stable manner along the accelerator. The boundary of the luminous zone begins to broaden and pulsate under these conditions. The plane structure of the stream irregularities is maintained far beyond the limits of the insulator.

Figure 9 shows the slit sweep 3 taken behind the end of the insulator. From this sweep it is evident that near the stream axis plane waves undergo stratification which is caused by the retardation of the stream during flow past the end of the insulator. The curving and stratification of the strips of irregularities substantiates the relationship between the irregularities and the stream and the influence of the gasdynamic action on the rotation of the stream behind the accelerator muzzle.

The artificial excitation of irregularities in a stream by the method described did not depend on the time elapsing between experiments (i.e., on the degree of deadsorption of gas by the electrodes).

The irregularities obtained in experiments with Plexiglas and Teflon adapters were practically identical. For a more refractory insulator, such as aluminum oxide, an increase in the frequency of the appearance of irregularities to 10-12 MHz was noted.

The artificial excitation of irregularities is accompanied by intense vaporization and a stream retardation which is greater than under conventional conditions (this is evident from the curves for the time variation of the velocity shown in Fig. 10). The velocity was determined according to the slope of the strips of the horizontal slit sweep on the axis of the model 1 (curve 1) and above the inner electrode of model 4 (curve 2). The difference in initial velocities can be explained by the retardation of the stream during flow past the end of the inner electrode in model 1. From Fig. 10 it follows that the vaporization of the insulator leads to a reduction of the stream velocity from $8 \cdot 10^6$ to $2 \cdot 10^6$ cm/sec. Since the vaporization process is distinguished by its inertia, it follows that the retardation of the stream and the appearance of irregularities have a certain time delay.

The reduction of the stream velocity allows the SFR streak camera to be used to obtain an overall photograph of the propagation of the irregularities. Several photographs from the frame-by-frame SFR photogram, as obtained behind the muzzle of model 4 having a Plexiglas adapter on the inner electrode, are shown in Fig. 11. The sequence of frames here is from the bottom up and from left to right. The photographing frequency was $3 \cdot 10^6$ frames/sec. The stream photographs which are given show that the irregularities have a flat axisymmetric shape, are generated in the zone between the end of the shock wave and insulator, and move with an interval of 3-4 cm, while expanding, along the stream at a velocity of the order of $2.5 \cdot 10^6$ cm/sec.

Thus, experiments on the artificial excitation of irregularities in a pulsed erosion accelerator have substantiated the assumption of the relationship of the irregularities mentioned in the paper given to viscid gasdynamic retardation of the stream, vaporization, and deadsorption on the surface of the electrodes.

LITERATURE CITED

1. I. F. Kvartskhava, R. D. Meladze, and K. V. Suladze, "Experiments on the electrodynamic acceleration of particles," Zh. Tekh. Fiz., 30, No. 3 (1960).
2. Yu. V. Skortsov, V. S. Komel'kov, and S. S. Tserevitinov, "Structure of magnetic fields in a plasma jet having eigencurrents," Zh. Tekh. Fiz., 34, No. 6 (1964).
3. V. N. Grigor'ev, "On the structure of plasmoids in an electrodynamic accelerator," Zh. Prikl. Mekh. i Tekh. Fiz., No. 2 (1965).
4. B. A. Osadin, "On the problem of forming plasmoids in a pulsed plasma accelerator," Zh. Tekh. Fiz., 35, No. 7 (1965).
5. V. A. Derevshchikov, "Measurement of the velocities of plasma components by means of streak photography in monochromatic light," Zh. Tekh. Fiz., 37, No. 2 (1967).
6. I. F. Kvartskhava, R. D. Meladze, É. Yu. Khautiev, N. G. Reshetnyak, and A. P. Sinyavskii, "On the causes of limitation of the velocity of plasmoids in railtrons," Zh. Tekh. Fiz., 34, No. 4 (1966).
7. O. K. Mawardi and M. Naraghi, "Measurements on current sheets in plasmas," IEEE Trans. Nucl. Sci., 10, No. 1 (1963).
8. A. M. Rushailo, "Measurement of thermal fluxes and estimation of the electrotemperature in a pulsed electromagnetic plasma accelerator," Zh. Prikl. Mekh. i Tekh. Fiz., No. 4, (1965).
9. A. M. Rushailo, "On thermal losses in a pulsed plasma accelerator," Zh. Prikl. Mekh. i Tekh. Fiz., No. 1 (1968).
10. L. E. Ivanova, "Investigation of the composition and distribution of the electron and ion temperatures over the cross section of a plasma jet behind the muzzle of a pulsed electromagnetic accelerator," Izvestiya Sib. Otdel. Akad. Nauk SSSR, No. 1 (1968).

11. Plasma Diagnostics [Russian translation], Mir, Moscow (1967).
12. G. M. Bam-Zelikovich, "The flow of a constructing gas in a jet behind the muzzle of an electromagnetic accelerator," Zh. Prikl. Mekh. i Tekh. Fiz., No. 1 (1967).
13. G. W. Satton and A. W. Carlson, "End effects in inviscid flow in a magnetohydrodynamic channel," J. Fluid. Mech., 11, No. 1 (1961).
14. M. A. Lavrent'ev and B. F. Shabat, Methods of the Theory of Functions of a Complex Variable [in Russian], Fizmatgiz, Moscow (1958).